Managed by Fermi Research Alliance, LLC for the U.S. Department of Energy Office of Science

Simulation of Particle-Material Interactions: 1. Basics

Nikolai Mokhov

CERN Accelerator School
Thessaloniki, Greece
November 11-23, 2018

This Course at CAS-Thessaloniki / Nov. 2018

- **Nov. 20: Simulation of Particle-Material Interactions: 1. Basics**
- Nov. 20: Simulation of Particle-Material Interactions: 2. Advanced Implementation in the Monte-Carlo Codes
- Nov. 22: Comparison of Various Codes for Particle Interaction with Material

Outline

- Introduction
- Interactions of Fast Particles with Matter
- Particle Transport Theory Essentials
- Monte-Carlo Method in Particle Transport in Matter
- Total and Differential Cross-sections and Event Generators
- Ready to Simulate Neutral Particle Interactions
- Response of Additive Detector
- Uncorrelated and Correlated Energy Loss and Scattering
- Decay of Unstable Particles

Introduction

The consequences of controlled and uncontrolled impacts of high-intensity or/and high-power or/and high-energy beams on components of accelerators, beamlines, target stations, beam collimators, absorbers, detectors, shielding, and environment can range from minor to catastrophic.

Strong, weak, electromagnetic and even gravitational forces (neutron oscillation and neutron TOF experiments) govern high-energy beam interactions with complex components in presence of electromagnetic fields ➔ simulations are only possible with a few well-established Monte-Carlo codes (no analytic or simplified approaches are used these days).

Predictive power and reliability of particle transport simulation tools and physics models in the multi-TeV region should be well-understood and justified to allow for viable designs of future colliders with a minimal risk and a reasonable safety margin.

Interactions of Fast Particles with Matter

Electromagnetic interactions, decays of unstable particles and strong inelastic and elastic nuclear interactions all affect the passage of high-energy particles through matter. At high energies the characteristic feature of the phenomenon is creation of hadronic cascades and electromagnetic showers (EMS) in matter due to multi-particle production in electromagnetic and strong nuclear interactions.

Because of consecutive multiplication, the interaction avalanche rapidly accrues, passes the maximum and then dies as a result of energy dissipation between the cascade particles and due to ionization energy loss. Energetic particles are concentrated around the projectile axis forming the shower core. Neutral particles (mainly neutrons) and photons dominate with a cascade development when energy drops below a few hundred MeV.

Microscopic View

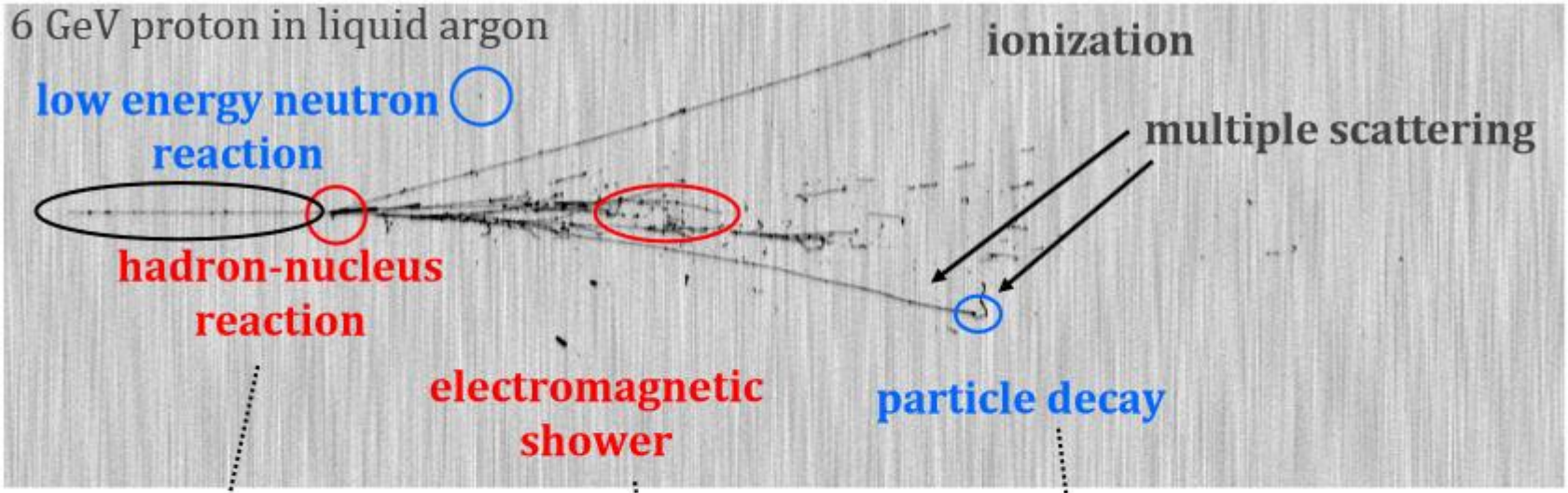

$$\lambda\rho = \frac{A}{\sigma_R N_A} \qquad \sigma_R \simeq \pi r_0^2 A^{2/3}$$

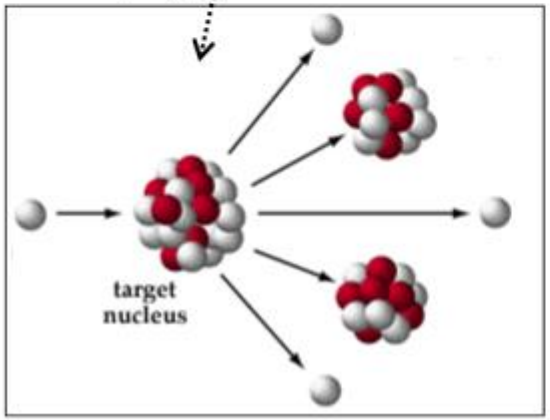

interplay of many physical processes described by different theories/models

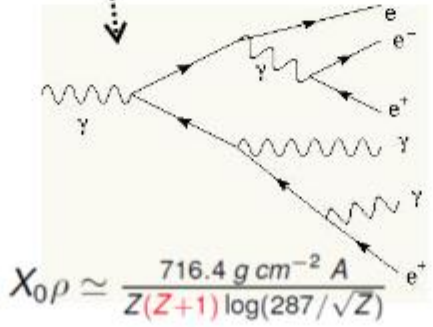

$$X_0\rho \simeq \frac{716.4\ g\ cm^{-2}\ A}{Z(Z+1)\log(287/\sqrt{Z})}$$

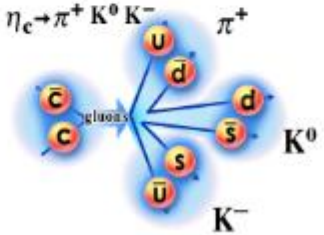

Fermilab

Scales of Cascades and Particle Propagation

The length scale in hadronic cascades is a nuclear interaction length λ_I (16.8 cm in iron) while in EMS it is a radiation length X_0 (1.76 cm in iron). The hadronic cascade longitudinal dimension is (5-10) λ_I, while in EMS it is (10-30) X_0. It grows logarithmically with primary energy in both cases. Transversely, the effective radius of hadronic cascade is about λ_I, while for EMS it is about $2r_M$, where r_M is a Moliere radius $R_M = 0.0265\ X_0\ (Z+1.2)$. Low-energy neutrons coupled to photons propagate much larger distance in matter around cascade core, both longitudinally and transversely, until they dissipate their energy in a region of a fraction of an electronvolt.

Muons - created predominantly in pion and kaon decays during the cascade development – can travel hundreds and thousands of meters in matter along the cascade axis. Neutrinos – usual muon partners in such decays – propagate even farther, hundreds and thousands of kilometers, until they exit the Earth's surface.

Materials Under Irradiation

Depending on material, level of energy deposition density and its time structure, one can face a variety of effects in materials under impact of directly particle beams or radiation induced by them.

Component damage (lifetime):

- Thermal shocks and quasi-instantaneous damage
- Insulation property deterioration due to dose buildup
- Radiation damage to inorganic materials due to atomic displacements and helium production

Operational (performance):

- Superconducting magnet quench
- Single-event upset and other soft errors in electronics
- Detector performance deterioration
- Radioactivation, prompt dose and impact on environment

Thermal Shock

Short pulses with energy deposition density EDD in the range from 200 J/g (W), 600 J/g (Cu), ~1 kJ/g (Ni, Inconel) to ~15 kJ/g: thermal shocks resulting in fast ablation and slower structural changes.

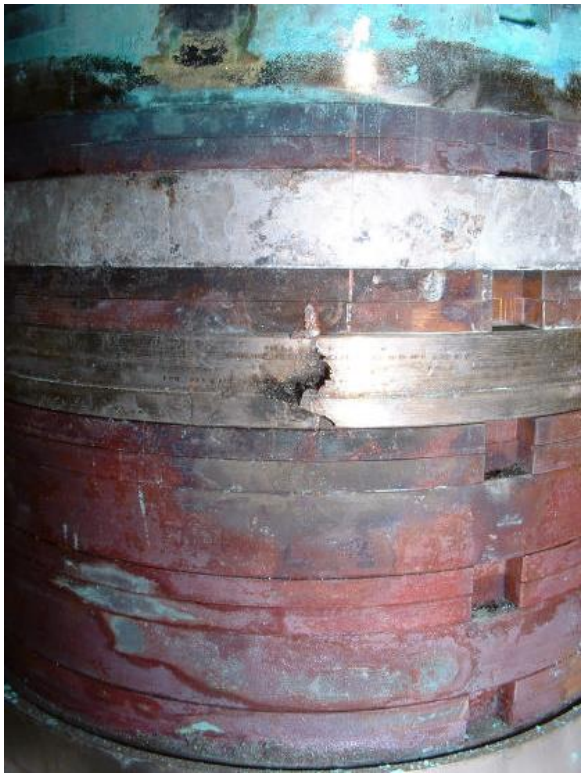

FNAL pbar production target under 120-GeV p-beam (3e12 ppp, σ ~ 0.2 mm)

MARS simulations explained target damage, reduction of pbar yield and justified better target materials

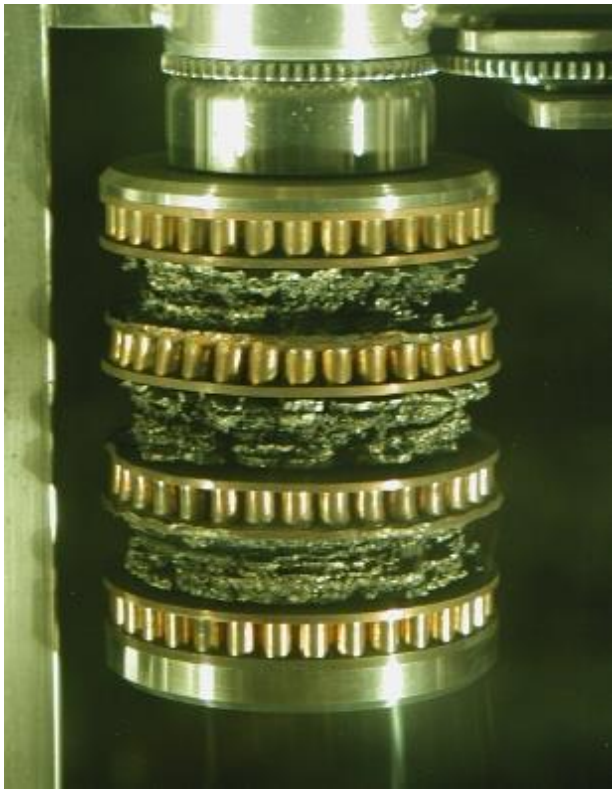

Particle Transport Theory Essentials

$N_i(\vec{r}, \vec{\Omega}, E, t)$: Differential in space, angle, energy and time density of particles of *i*-type in a unit phase volume near a phase point $\mathbf{x} = (\vec{r}, \vec{\Omega}, E, t)$. Below we use $N = N_i$.

Let's consider elemental area dS centered at a point $\vec{r}$ and having normal vector $\vec{\mathrm{n}}$. For a time interval dt, the area can be crossed by particles contained in the volume $dV = |\vec{v}\,\vec{n}|\, dS\, dt = |\vec{\Omega}\,\vec{n}|\, v\, dS\, dt$, where $\vec{v} = v\vec{\Omega}$ is a velocity of a particle corresponding to its energy E. A number of such particles is

$$N(\mathbf{x}, t)\, dV = \vec{\Omega}\,\vec{\mathrm{n}}\ \Phi(\vec{r}, \vec{\Omega}, E, t)\, dS\, dt\ ,$$

where function $\Phi(\vec{r}, \vec{\Omega}, E, t) = v\, N(\vec{r}, \vec{\Omega}, E, t)$ is ***differential flux density*** for particles of *i*-type. Again, we use here $\Phi = \Phi_i$. Many other characteristics used in transport theory can be derived from $\Phi(\mathbf{x})$.

Frequently Used Functionals of Φ

$\Phi(\vec{r},\vec{\Omega},t) = \int_0^\infty \Phi(\vec{r},\vec{\Omega},E,t)dE$ *is spatial-angular flux density*

$\Phi(\vec{r},E,t) = \int_{4\pi} \Phi(\vec{r},\vec{\Omega},E,t)d\vec{\Omega}$ *is spatial-energy flux density*

$\Phi(\vec{r},t) = \int_0^\infty \Phi(\vec{r},E,t)dE = \int_{4\pi} \Phi(\vec{r},\vec{\Omega},t)d\vec{\Omega}$ *is flux density*

$\Phi(\vec{r}) = \int_0^\infty \Phi(\vec{r},t)dt$ *is particle fluence*

$\Phi(t) = \int \Phi(\vec{r},t)d\vec{r}$ *is particle flux*

$E\Phi(\vec{r},\vec{\Omega},E,t)$ is *differential energy flux density*

$\vec{\Omega}\Phi(\vec{r},\vec{\Omega},E,t)$ is *differential current density*

$S(\vec{r},\vec{\Omega},E,t) = \Sigma(\vec{r},E)\ \Phi(\vec{r},\vec{\Omega},E,t)$ is *differential collision (absorption, scattering) density, where* $\Sigma(\vec{r},E)$ *is collision (absorption, scattering) macroscopic cross-section,* $\Sigma(\vec{r},E) = 1/\lambda(\vec{r},E)$ *where* $\lambda(\vec{r},E)$ *is particle mean free-path*

$S(\vec{r}\,)$ is often called *particle star density* or density of inelastic nuclear interactions, if $\Sigma(\vec{r})$ is macroscopic absorption x-section

Bolzmann Kinetic Equation of Particle Transport

$\Phi(\vec{r},\vec{\Omega},E,t)$ obeys the system of Boltzmann equations which are derived from a balance of particles of *i*-type (index *i* is skipped again) incoming to and leaving from a unit phase space along with creation and absorption:

$$\frac{1}{v}\frac{\partial}{\partial t}\Phi(\vec{r},\vec{\Omega},E,t)+\vec{\Omega}\,\vec{\nabla}\Phi(\vec{r},\vec{\Omega},E,t)+\boldsymbol{\Sigma}(\vec{\boldsymbol{r}},\boldsymbol{E})\Phi(\vec{r},\vec{\Omega},E,t)=$$
$$\sum_j\int d\Omega'\int dE'\,\Sigma\left(\vec{r},\vec{\Omega'}\to\vec{\Omega},E'\to E\right)\Phi_j(\vec{r},\vec{\Omega},E,t)+\mathrm{G}\,(\vec{r},\vec{\Omega},E,t) \quad (1)$$

where

$\boldsymbol{\Sigma}(\vec{\boldsymbol{r}},\boldsymbol{E})$ is a ***total macroscopic cross-section*** for the given particle type (*i*); in addition to nuclear interaction, it can include the decay one for unstable particles $\Sigma_D\,(E)=1/\lambda_D(E)=m/(c\tau p)$ and ionization loss one for charged particles $-\frac{\partial}{\partial E}\frac{dE}{dx}(\vec{r},E)/\rho(\vec{r})$

$\Sigma(\vec{r},\Omega'\to\Omega,E'\to E)$ is a ***double-differential cross-section*** which defines creation of particles of *i*-type in the end state $\vec{\Omega},E$ from the initial state $\vec{\Omega'},E'$ by all types j of particles under consideration

$\mathrm{G}(\vec{r},\vec{\Omega},E,t)$ is the density of the external sources

Deterministic Methods

The Bolzmann equations were successfully used for decades in reactor applications for neutrons and photons in 1D, 2D and even 3D cases applying deterministic transport methods for the average particle behavior (most common of which was the discrete ordinate method).

Starting early 60's, several attempts have been undertaken to solve the system of transport equations at high energies for – as called at that time - "nucleon-meson cascades". Special forms of the $\Sigma(\vec{r}, \Omega' \rightarrow \Omega, E' \rightarrow$

From Deterministic to Monte-Carlo Methods

It has become clear that the general case of the hadronic-electromagnetic cascades with all the known elementary particles and products of nuclear reactions can only be solved using Monte-Carlo methods.

The general case includes all the correlations at the interaction vertices over the energy range of, say, 10^{14} decades, with cascades developed in complex 3D geometry of nuclear and accelerator facilities, experimental setups and their detectors, with magnetic fields etc.

Monte-Carlo Method in Particle Transport in Matter

Nowadays, the **Monte-Carlo method (MCM)** is the principal, if not the only, method in particle transport applications. In its simplest and at the same time most dependable and common form – ***direct mathematical modeling*** – it involves numerical simulation of the interactions and propagation of particles in matter. In this approach, all the physics processes are modelled as these take place in the real world, in realistic geometry and fields of accelerators and experimental setups.

The use of various modifications of MCM, the so--called ***variance reduction techniques***, makes it possible to greatly simplify the solution of the problem in certain cases, with a very high accuracy reached in a limited phase space volume.

MCM Basics: Sampling Random Quantities (1)

The random continuous quantity ξ is determined in the interval (a, b) by the function $p(x)$, which is called the ***probability density***. The probability that ξ will be in the interval (a, x) is $P(a < \xi < x) = \int_a^x p(x')dx'$, where $p(x) > 0$ and $\int_a^b p(x)dx = 1$. (2)

The expectation value of ξ (its ***mean value***) is $\boldsymbol{M}\xi = \int_a^b xp(x)dx$. For random continuous function $f(x)$, $\boldsymbol{M}f(\xi) = \int_a^b f(x)p(x)dx$.

MCM Basics: Sampling Random Quantities (2)

With a generator of random numbers γ, which are uniformly distributed in the interval $(0,1)$, the use of the equation $\gamma = P(x) = \int_a^x p(x')dx'$ allows us to randomly chose the values $x = P^{-1}(\gamma)$. This the ***inverse-function method*** used when the integral can be expressed in terms of the elementary functions. Otherwise, the ***Neumann (or rejection) method*** can be used: the density function of ξ $(a < \xi < b)$ is redefined as follows $p^*(x) = \frac{p(x)}{Max[p(x)]}$. Choose two random numbers, γ_1 and γ_2, and calculate $x' = a + \gamma_1(b - a)$.

If $\gamma_2 < p^*(x')$, $\xi = x'$. Otherwise, the (γ_1, γ_2) pair is discarded, a new pair is chosen and the procedure is repeated.

Find the area (volume) of an arbitrary shape ➔ how MCM was born

Nuclear Interaction Cross-Sections

The **first most important quantity** to solve the equation (1) or simulate particle transport by Monte-Carlo method

$$\Sigma(i,A,E) = \frac{\sigma(i,A,E) N_A \, 10^{-27} \, \rho}{A}, \text{ cm}^{-1}$$

where σ is a microscopic x-section (mb) for a given interaction type of a particle of *i*-type with a chosen absorber nucleus with atomic mass A; N_A is Avogadro number (=6.022 × 10^{23} mol^{-1}), ρ is density (g/cm^3)

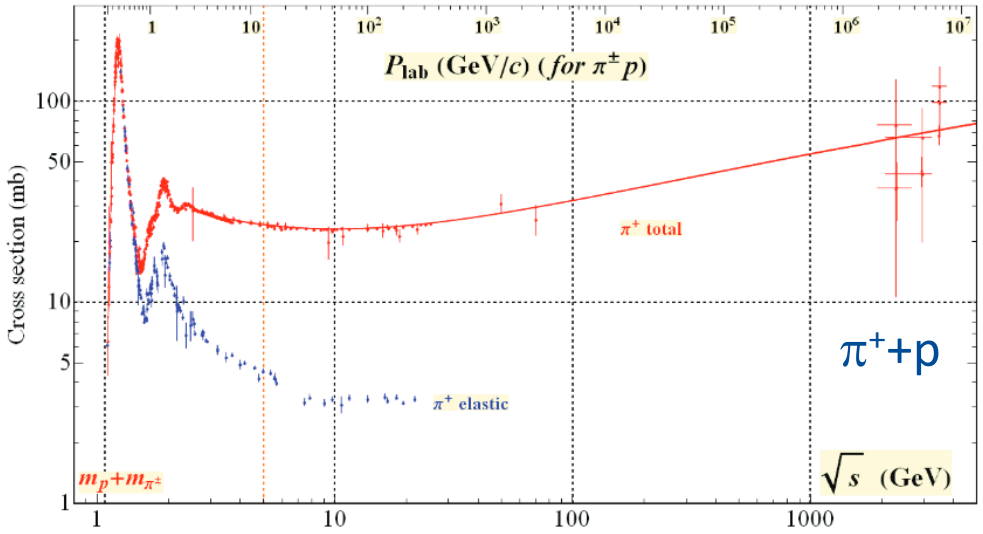

$$s = m_1^2 + m_2^2 + 2E_{1lab}m_2$$

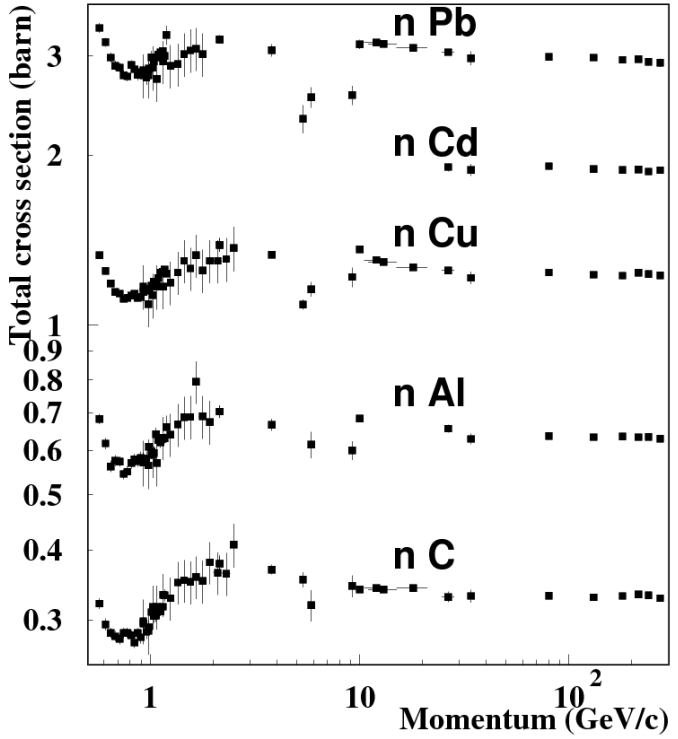

Fermilab

Low-Energy Neutron-Nucleus Cross-Sections

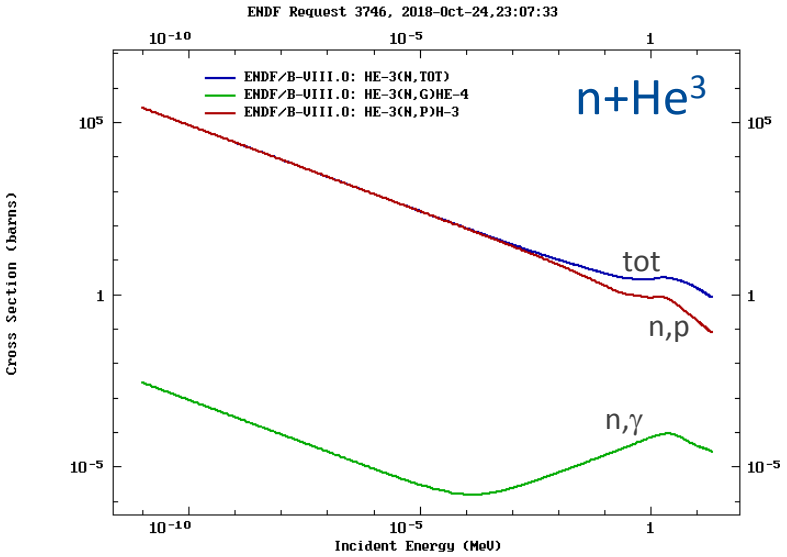

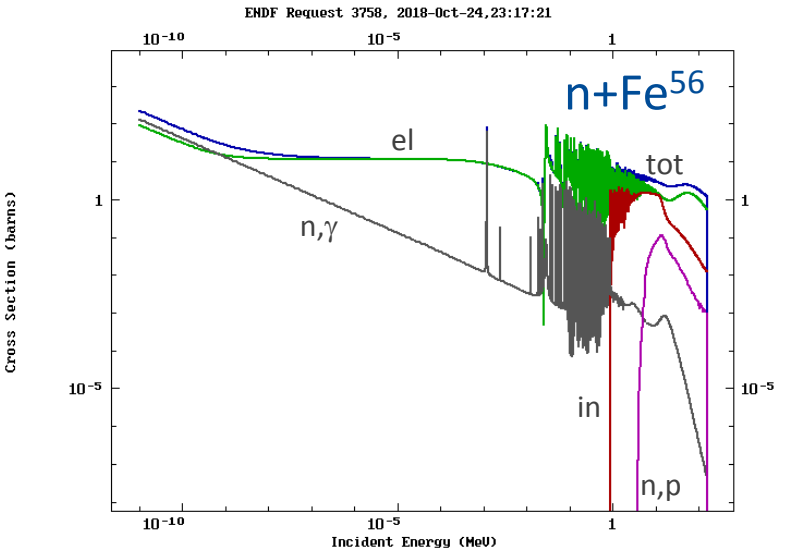

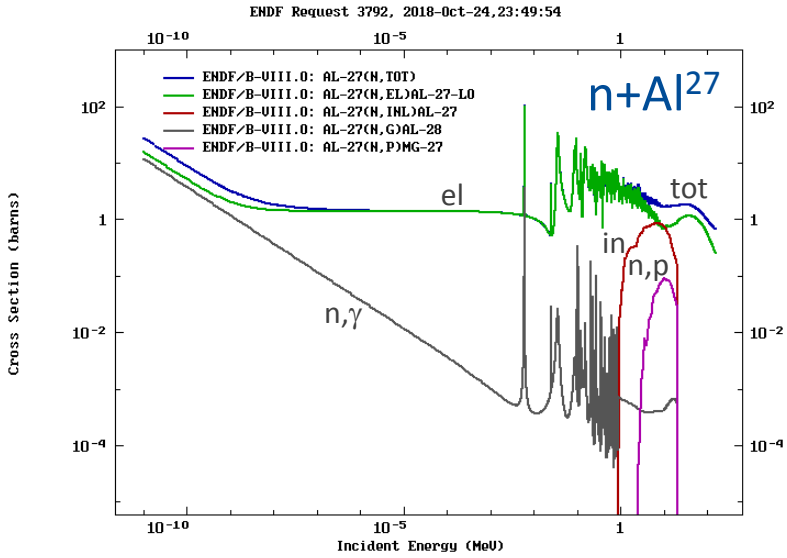

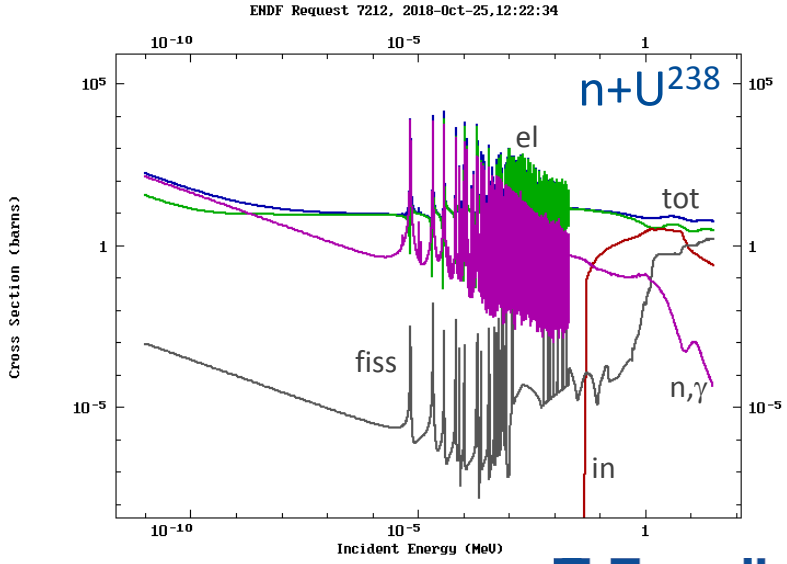

Fermilab

Double-Differential X-Section or Particle Production Models

The **second most important quantity** to solve the equation (1) or simulate particle transport by Monte-Carlo method is a double-differential cross-section:

$$\Sigma(\vec{r}, \Omega' \to \Omega, E' \to E) = \frac{d^2\sigma(i,j,A,E',E,\Omega',\Omega)}{dEd\Omega} \times \frac{N_A 10^{-27} \rho}{A}$$

It can be taken from pre-calculated databases (e.g., ENDF for low-energy neutrons with their x-section resonant structure), or some theoretical forms allowing - in simplest cases - even analytical solutions.

At high-energies, a standard approach nowadays is to use ***event generators***, performing Monte-Carlo simulation through all the stages of particle interactions inside a nucleus like a quark-gluon cascade, hadron intranuclear cascade, preequilibrium stage, evaporation/fragmentation and gamma-deexcitation. This is realized in DPMJET (Dual Parton Model), FRITIOF (string model), LAQGSM (quark-gluon string model), QMD (Quantum Molecular Dynamics model) and other theoretical models and codes.

Statistical Weights and Inclusive Sampling (1)

In contrast with the transport of low- and intermediate energy hadrons through matter, a high-energy hadron cascade is a strongly branching process because of the multiple production of particles in the nuclear *hA* interactions at energies above 10-30 GeV. Besides, the earlier theoretical models for high-energy particle-nuclear interactions suffered from a number of inconsistencies.

These factors – along with a limited computing power in 70's – forced developments of inclusive schemes for particle production in *hA* interactions based on the method of ***statistical weights***.

Statistical Weights and Inclusive Sampling (2)

In its original simplest form, one generates at each vertex only one "representative" sampled particle which carries a ***statistical weight W*** equal to the total multiplicity at such a vertex. The functionals are conserved in such an approach on average, but correlations are lost.

One can multiply and divide the integrand $\Sigma(x)$ in Eq. (1) by a function $p(x)$ of Eq. (2) to simplify the sampling and populate a region of interest. Latter is the basis of a widely used these days the variance reduction techniques.

$\Phi = \int \Sigma(x)dx$ ➔ $\Phi = \int W(x)p(x)dx$

where $x = (E, \mathbf{\Omega})$ and $W(x) = \Sigma(x)/p(x)$ is a statistical weight

$$\Phi_N = \frac{1}{N}\sum_{k=1}^{N} W(x_k)dl_k/dVk$$

EMS simulation in exclusive (analogue) and simplest inclusive (statistical weight) schemes:

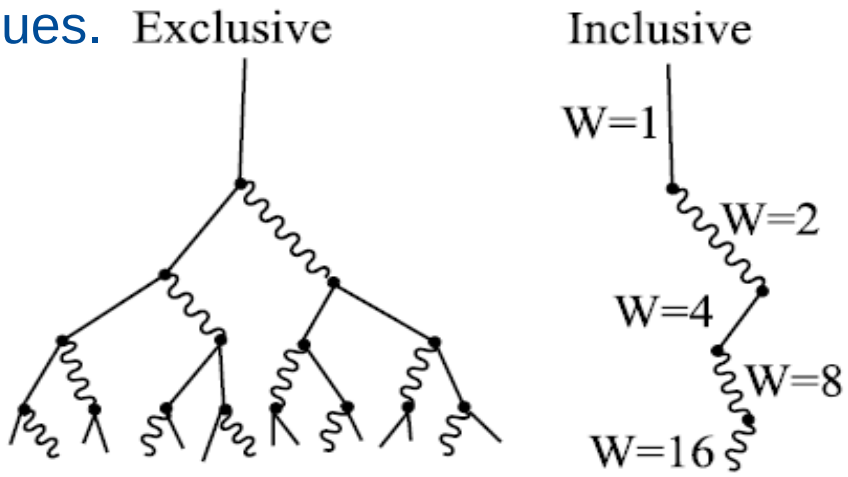

Fermilab

Semi-Inclusive hA Vertex at E > 5 GeV

The hA vertex can be built to better match the needs of a specific application. The following scheme provides a high efficiency $\varepsilon = (t\,\sigma^2)^{-1}$ in accelerator and shielding applications. Here t is the CPU time needed to reach a statistical RMS error of σ. The statistical weights attached to each particle guarantee that the results are unbiased.

Note:
A combination of exclusive, semi-inclusive and inclusive sampling in the same session can provide the best efficiency in the given application.

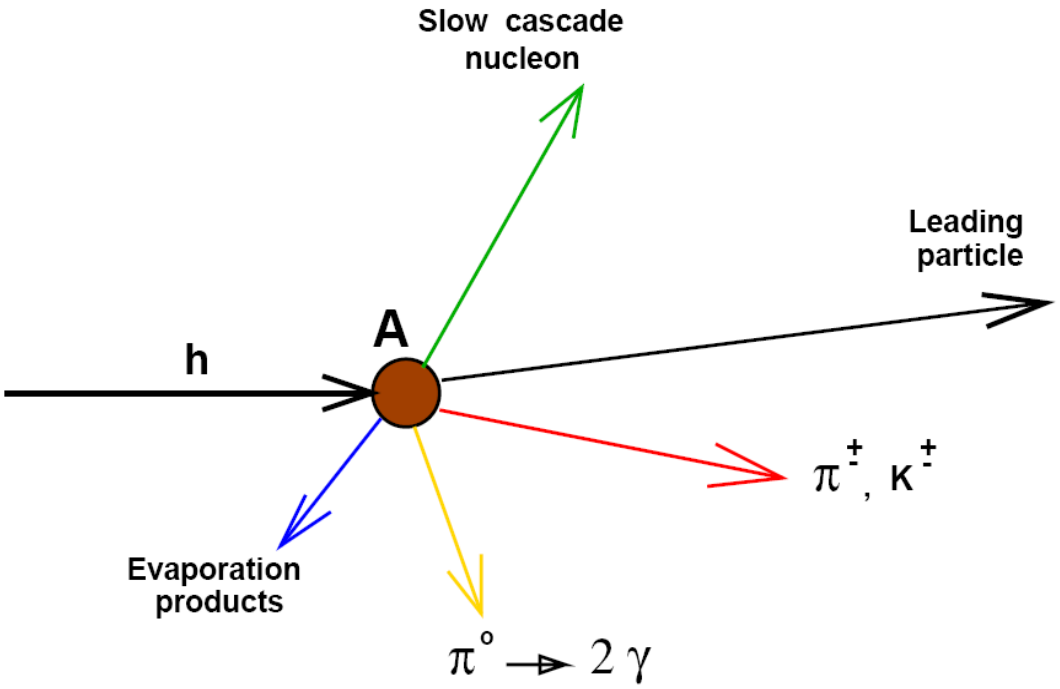

Hadron Vertex: Exclusive *vs* Semi-Inclusive

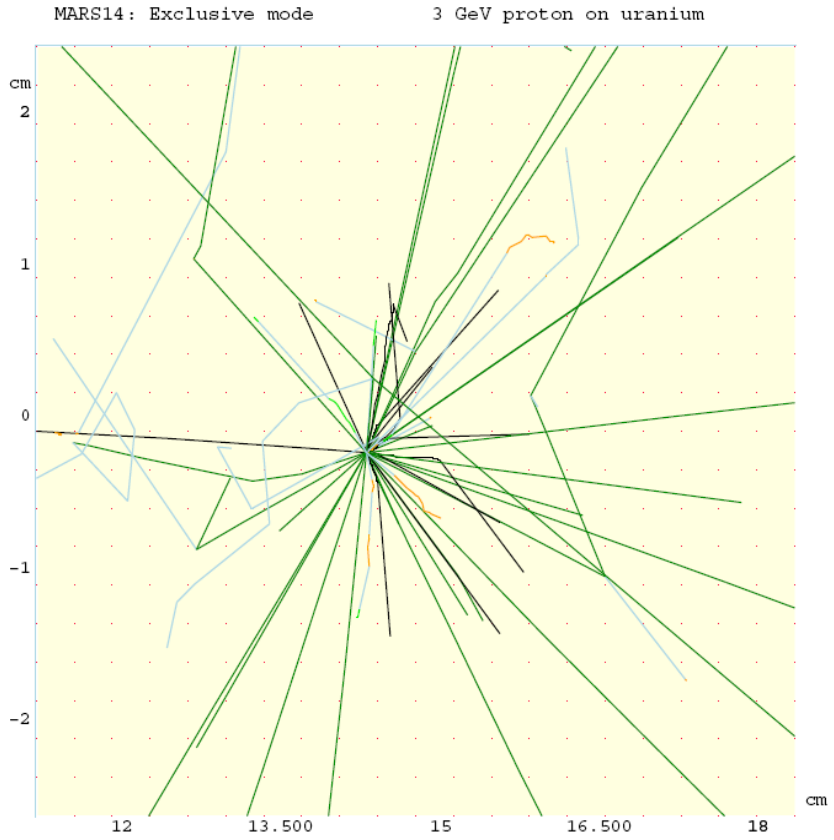

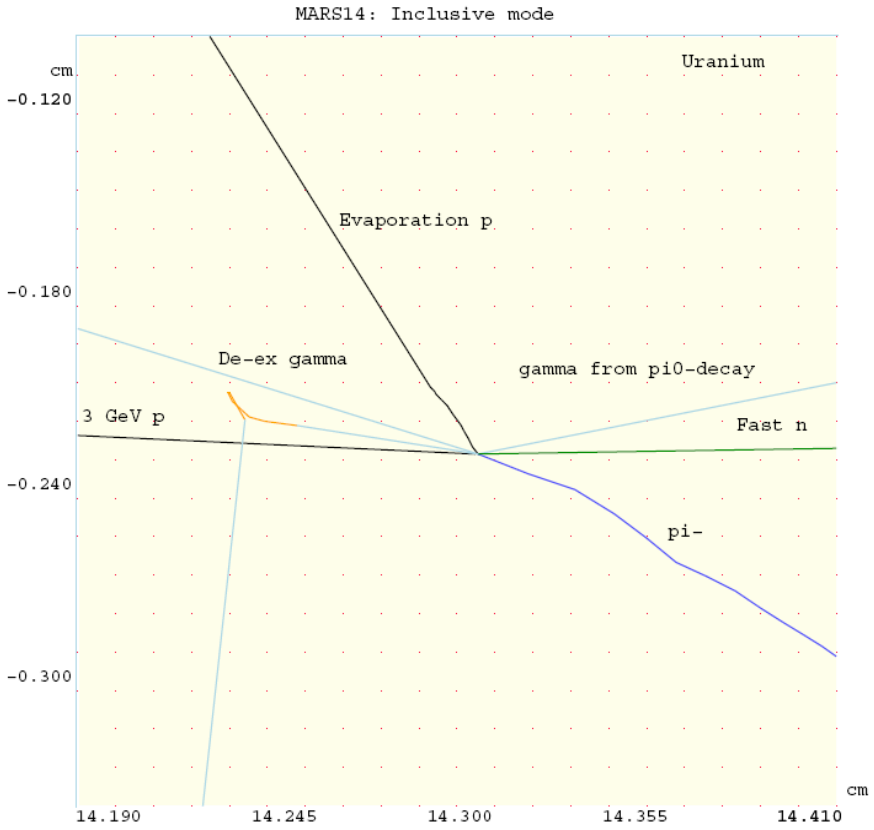

3-GeV proton on 20-cm uranium target

Fermilab

Example of a Nuclear Event Generator Set

- Projectile E_0 < 0.12 GeV down to 1 MeV (charged particles) and 14 MeV (neutrons): a combination of extended TENDL-2016 (inclusive, semi-inclusive or exclusive mode – user's choice) and LAQGSM
- 0.12 < E_0 < 0.5 GeV: a combination of CEM-2018 and LAQGSM-2018
- 0.5 < E_0 < 10 GeV: LAQGSM
- 10 GeV < E_0 < 100 TeV: LAQGSM or inclusive (user's choice)

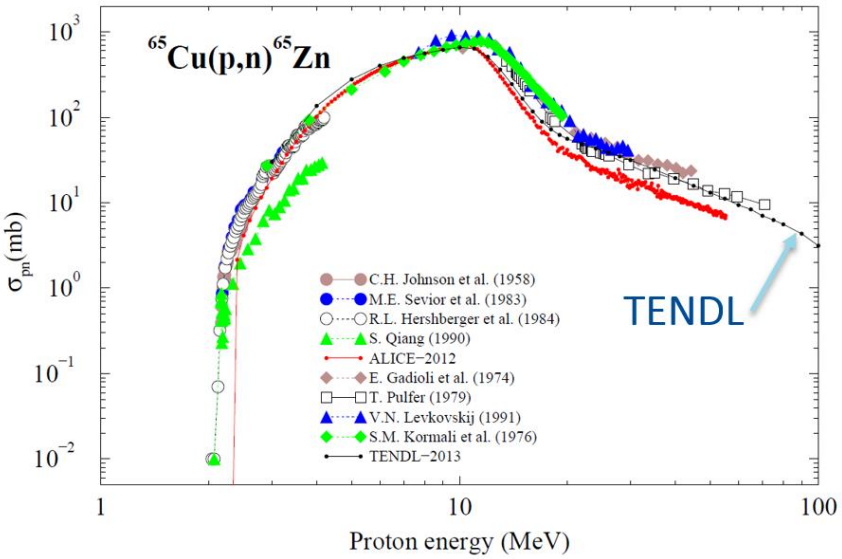

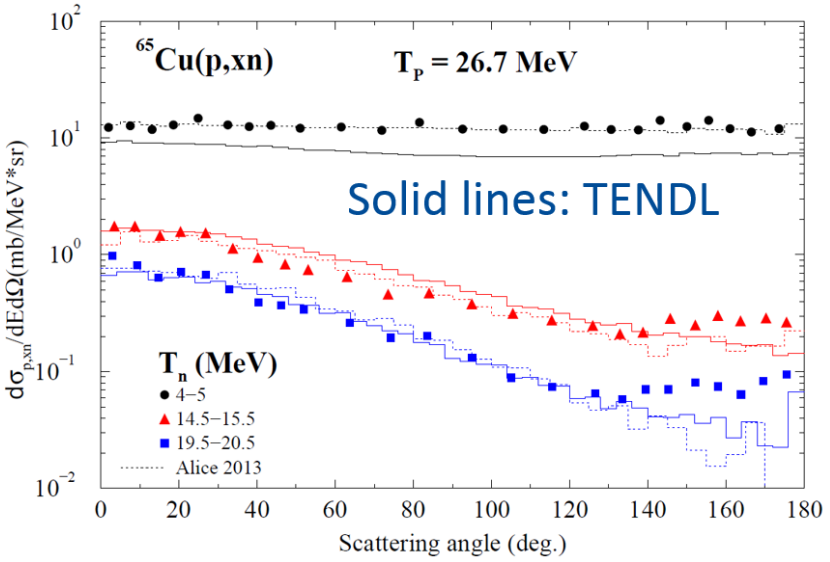

LAQGSM Performance at 585 and 730 MeV

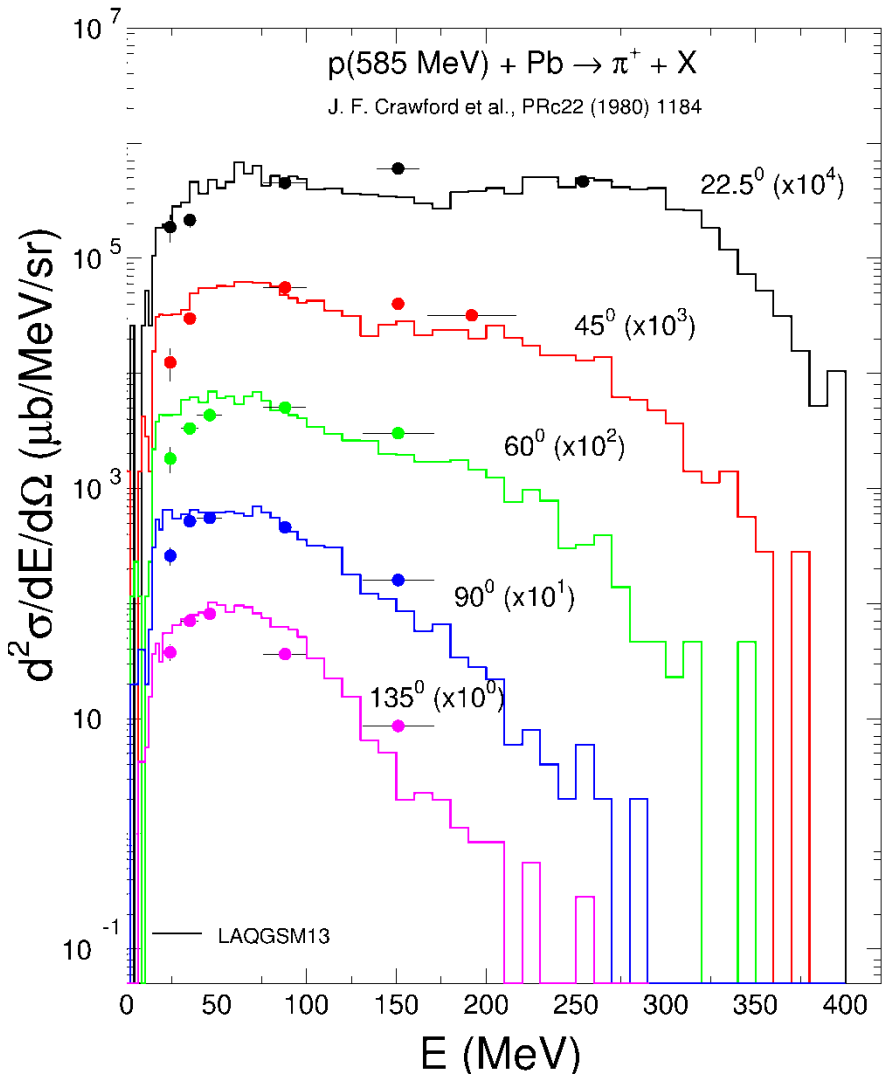

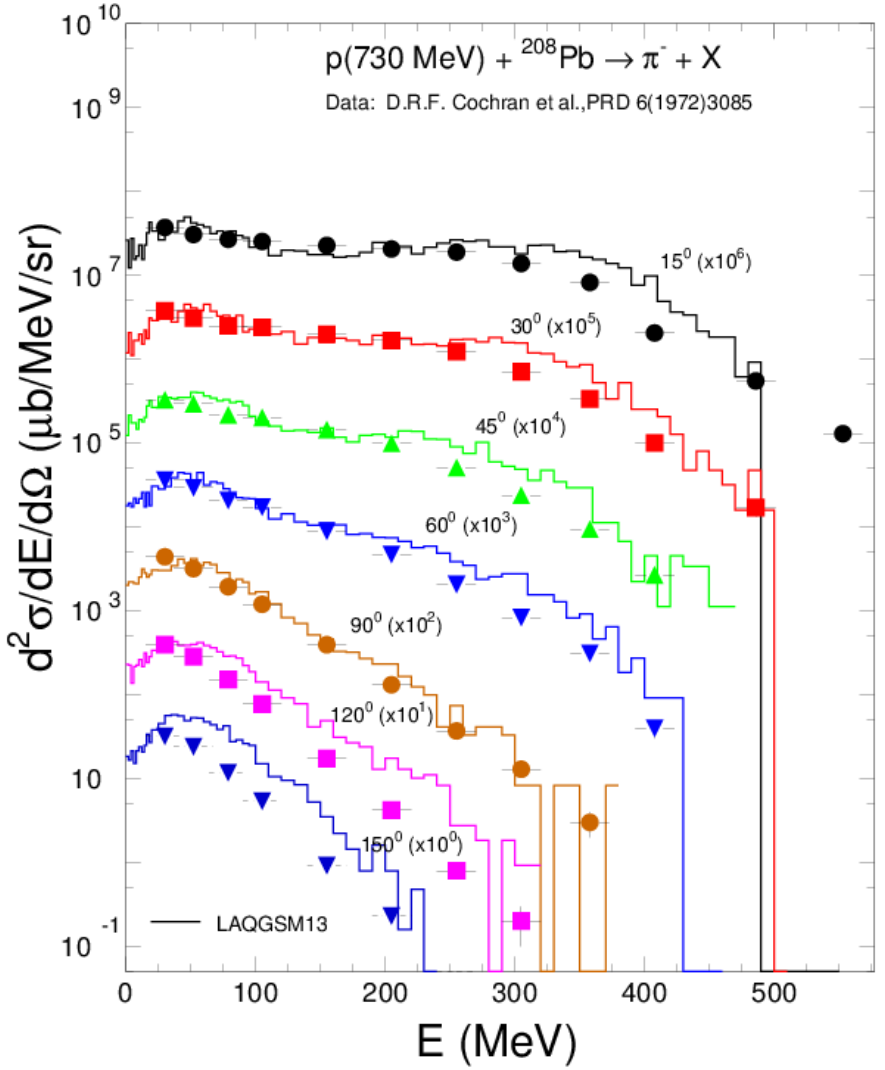

LAQGSM vs HARP-CDP at 8GeV/c and KaoS at 3.5GeV

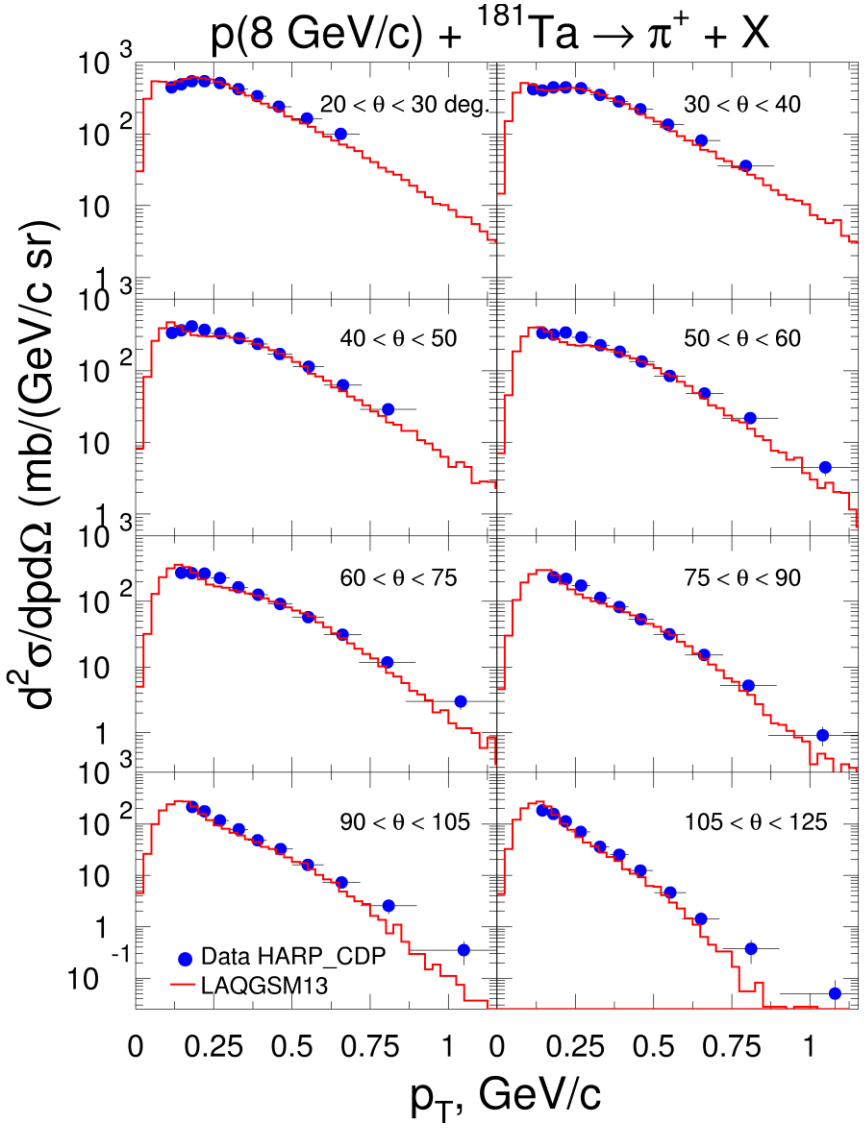

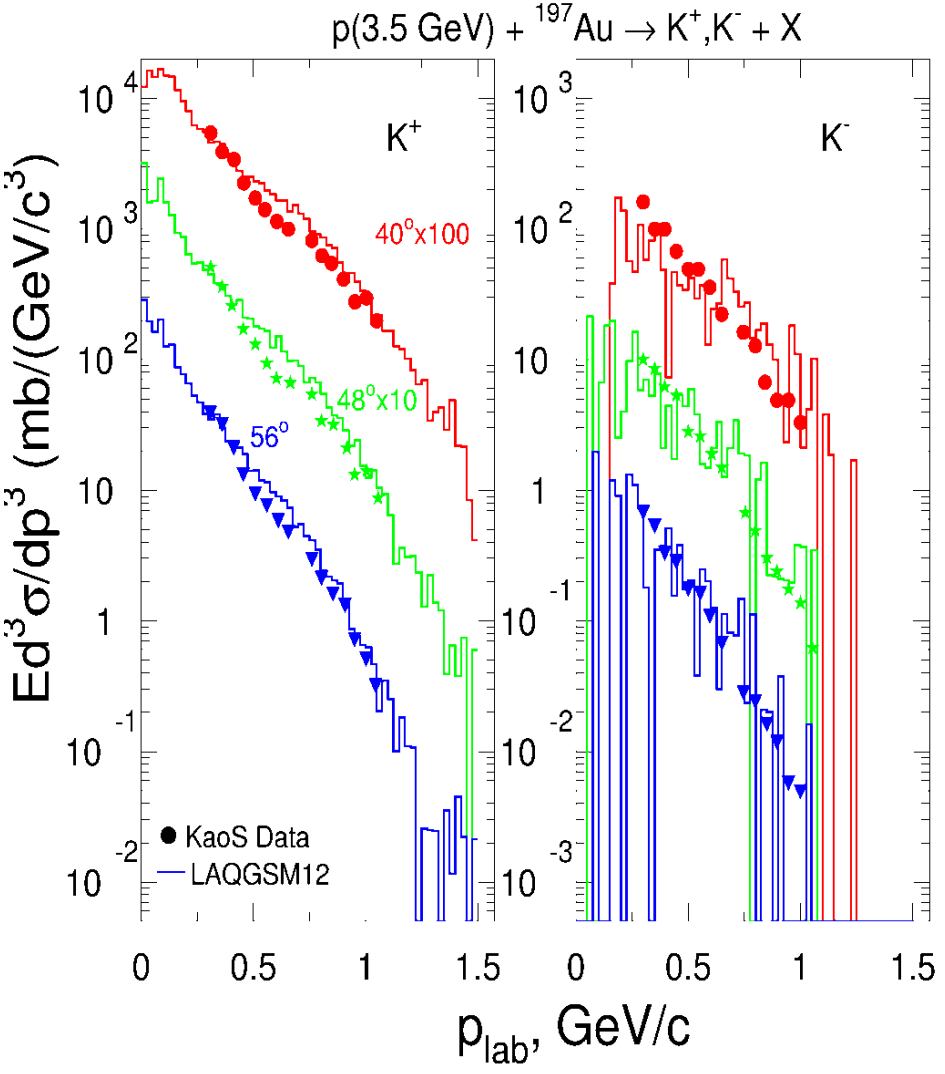

Fermilab

Newest DPMJET III and FLUKA's EMD *vs* LHC Data

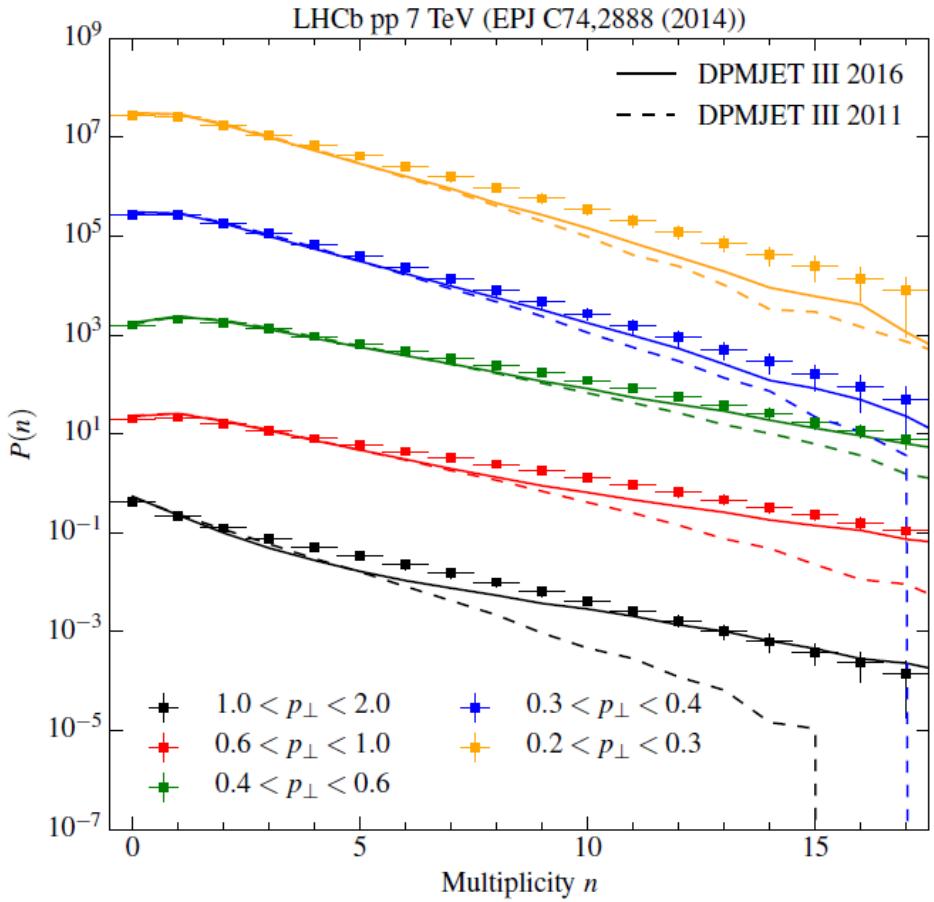

Charged particle multiplicity in pp-collisions at $\sqrt{s}$ = 7 TeV integrated over η = 2 - 4.5 as measured by LHCb (symbols) and simulated with DPMJET-III

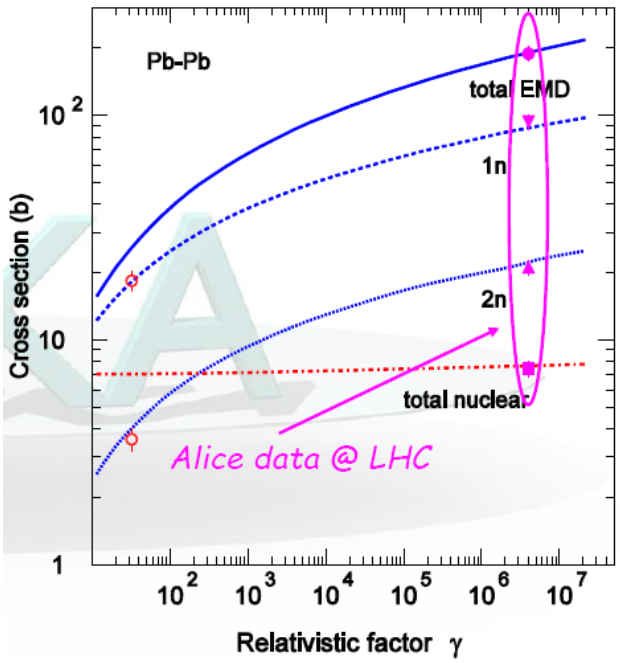

Electromagnetic dissociation (EMD) and nuclear x-sections in Pb-Pb collisions: FLUKA *vs* ALICE data. EMD = very peripheral nuclear interactions thru time-dependent EM field caused by moving nuclei. 1n – one-phonon GDR (high-frequency collective excitation of atomic nuclei, 2n – DGDR (double-phonon giant dipole resonance)

Courtesy A. Ferrari & A. Fedynitch

Nuclides from FLUKA & MARS15 Event Generators

FLUKA: 1 GeV/A ^{208}Pb + p

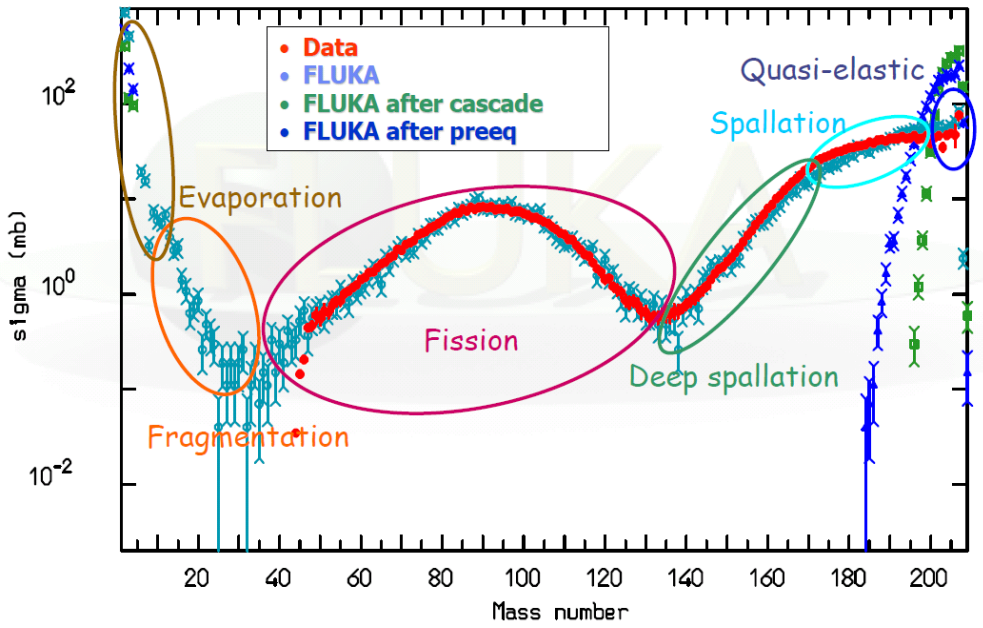

Production of residuals is the result of the last step of the nuclear reaction

MARS-LAQGSM

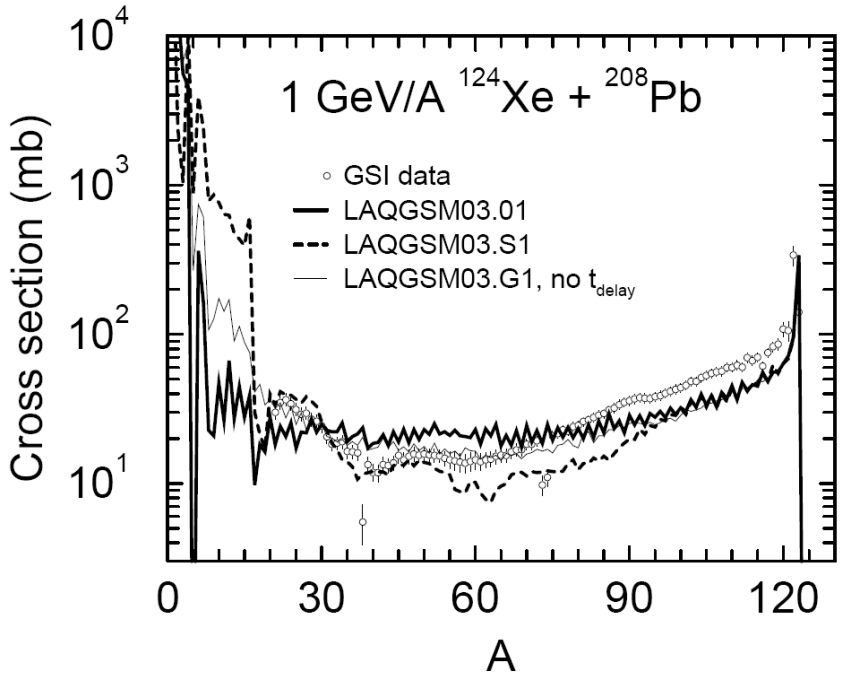

Fermilab

Exclusive and Inclusive EMS Simulation

1-GeV positron on 2-cm tungsten target

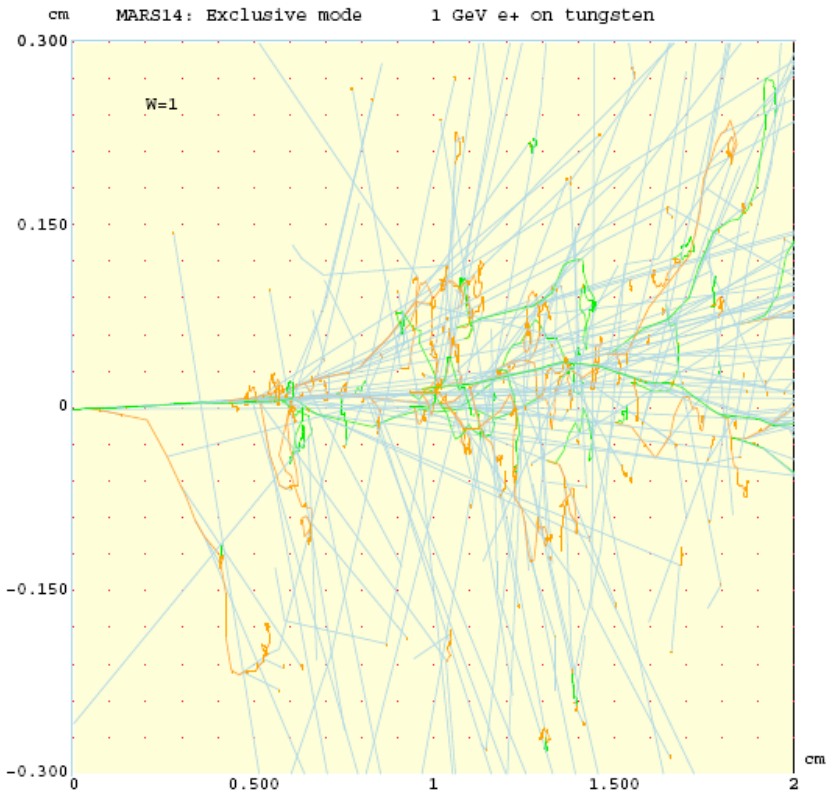

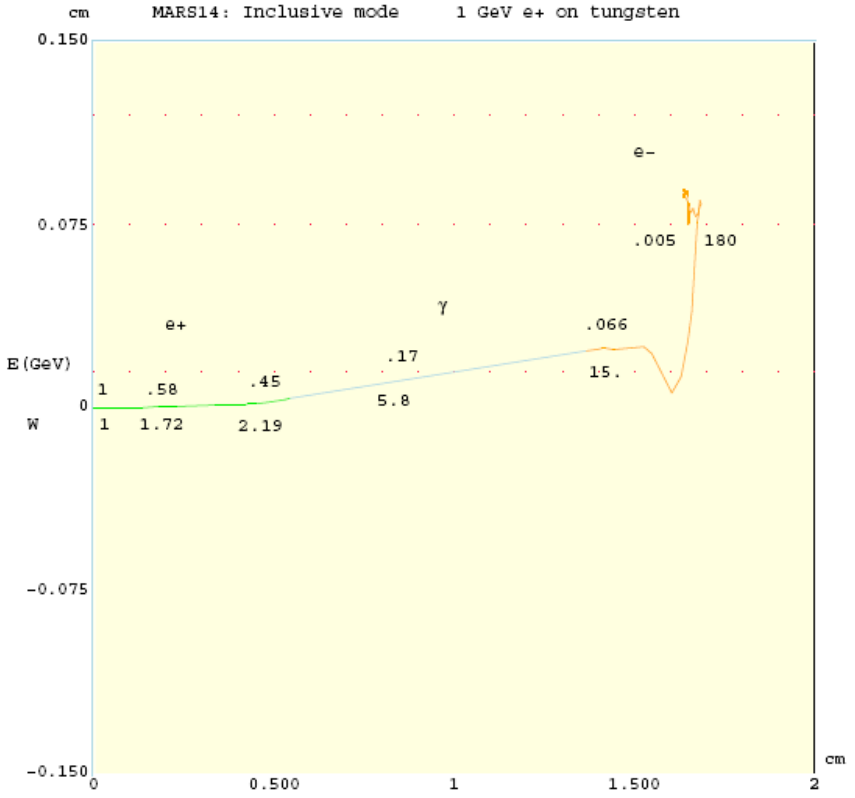

Fermilab

Inclusive, Exclusive and Hybrid EMS Simulations

One 10-GeV e^+ on 3cm W + 17cm concrete

Inclusive

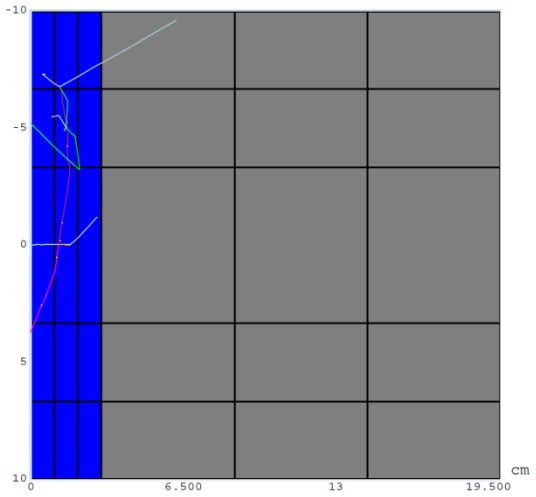

Hybrid-10

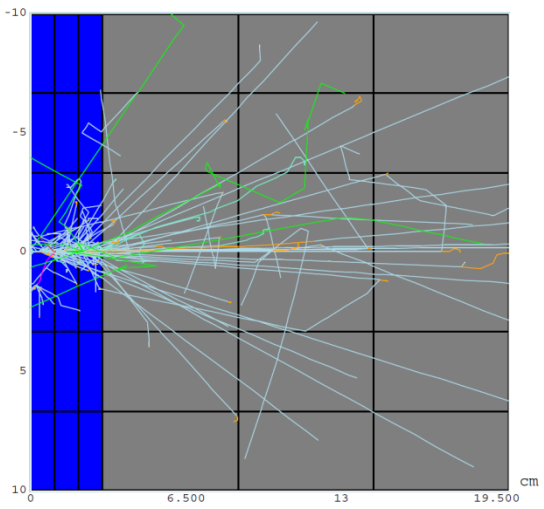

Exclusive

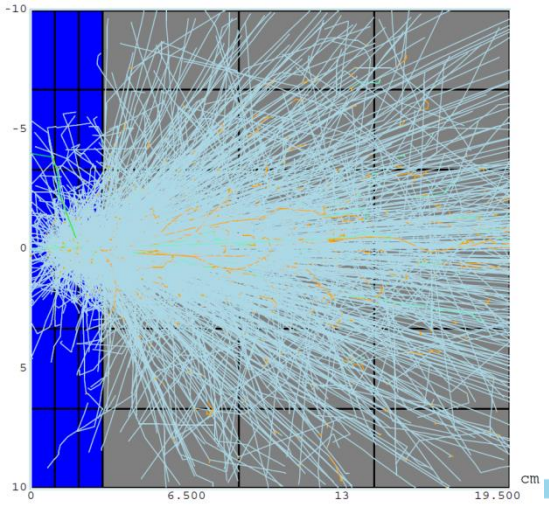

Hybrid-20

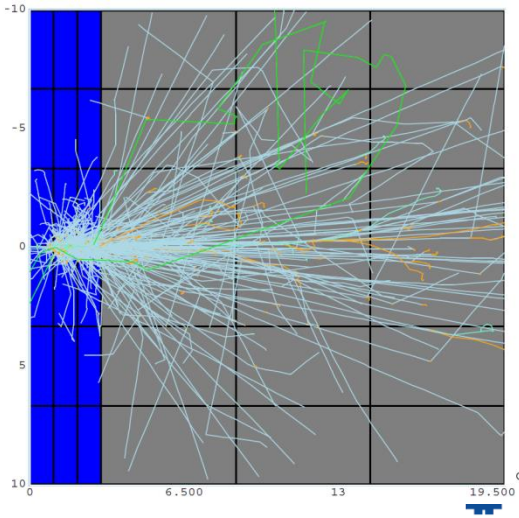

Fermilab

Ready for Simulation of Neutral Stable Particle Interactions in a Uniform Block

The range of a particle, R, before its discrete interaction is found by solving equation (1) whose right side is zero. In a coordinate system associated with the particle, its solution for neutral particles is $\Phi = \Phi_0 \exp(-\Sigma R)$. The corresponding probability density is $p(r) = \exp(-r)$, where $r = \Sigma$R. As shown in the MC method basic slides, the algorithm for simulating the range of R of neutral particles before their interaction: $r = -\ln(1-\gamma)$ or $R = -\Sigma^{-1}\ln(1-\gamma)$. The radius vector of the new interaction point can be determined now from the previous coordinates $\boldsymbol{r_0}$ as $r = \boldsymbol{r_0} + R\boldsymbol{\Omega}$. The ratio of a specific channel x-section to the total x-section, gives us a probability of this channel to take place. Sampling it and applying a corresponding algorithm for sampling type, energy and direction of generated secondary particles (database or event generator), we are equipped for simulation of processes initiated by a neutral particle in a uniform system. Adding a detector response (next slide) we are ready to go.

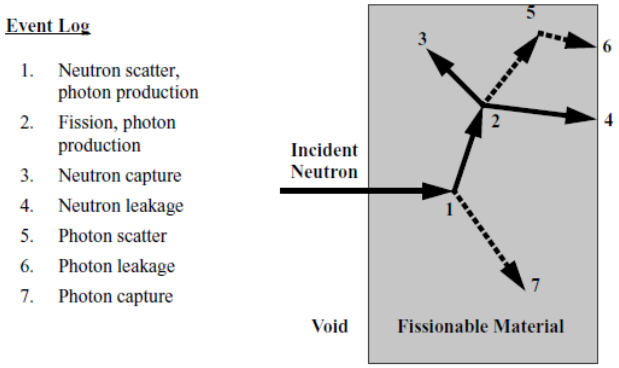

Channel sampling example

$\sigma_t = \sigma_1 + \sigma_2 + \sigma_3$, with $\gamma \in (0,1)$:

$\gamma < \sigma_1 / \sigma_t \Longrightarrow$ Channel 1

$\gamma < (\sigma_1 + \sigma_2) / \sigma_t \Longrightarrow$ Channel 2

otherwise $\Longrightarrow$ Channel 3

Fermilab

Response of Additive Detector

If the differential flux density is known, the reading (response) of any additive detector (in the broad sense) can be represented as

$$Res(t) = \iiint D\left(\vec{r}, \vec{\Omega}, E, t\right) \Phi\left(\vec{r}, \vec{\Omega}, E, t\right) d\vec{r}\, d\vec{\Omega}\, dE \qquad (3)$$

where $D\left(\vec{r}, \vec{\Omega}, E, t\right)$ is the sensitivity function of the detector, e.g., a light yield in scintillator. This is the average contribution to the detector readings from a unit path length of the particle with the coordinates $\left(\vec{r}, \vec{\Omega}, E, t\right)$ in the detector volume. Hence, the ***alternative definition of the differential flux density*** (with $D(\boldsymbol{x}) = 1$) as a quotient of the sum of the particle track length segments dl_k in the spatial volume dV of a phase volume near a phase point $\boldsymbol{x} = \left(\vec{r}, \vec{\Omega}, E, t\right)$ is $\Phi(\boldsymbol{x}) = \sum_k dl_k / dV$. Related ***energy deposition*** (with $D(\boldsymbol{x}) = dE$) for charged particles in dV is $\varepsilon(\boldsymbol{x}) = \sum_k dE_k dl_k / dV$.

Both are ready for prompt use in Monte-Carlo ***track length estimate.***

Monte-Carlo Simulation Scheme

The particles produced at the discrete interaction vertex are placed to the history bank, with one of them taken for the further transport to a new interaction point using the same techniques described in the previous slides. It is done with allowance for the particular features of the system (complex geometry, nonuniform material distribution, composite materials), decay of unstable particles, the possible quasi-continuous effects of the electromagnetic processes (ionization and radiative energy loss and multiple Coulomb scattering) and impact of magnetic and electric fields.

Virtually any functional of the random quantities ξ can be found directly during the simulation. The simulation of the history ends when the bank is empty and all the particles are absorbed or emitted from the system. The simulation is then repeated N times until the required statistical accuracy of the functionals is reached.

Statistical Accuracy

According to the central limit theorem, for large values of N, the distribution of the sum $\sum_{n=1}^{N} \xi_n$ is approximately normal. The following relation is therefore used to estimate the functional Φ

$$P\left\{abs\left(\frac{1}{N}\sum_{n=1}^{N}\xi_n - \Phi\right) < \delta\right\} \approx 0.997$$

This relation shows that – with a probability $P \cong 0.997$ - the error of the estimate is no greater than $\delta = 3\sqrt{D\xi/N}$, where $D\xi = \boldsymbol{M}(\xi^2) - (\boldsymbol{M}\xi)^2$, called a dispersion. That is, to calculate a statistical error of $\boldsymbol{M}\xi$, one sums ξ^2 - in the course of Monte Carlo session - along with summing random quantities ξ.

Quasi-Continuous Effects

To account for quasi-continuous effects in MCM, the charged particle path-length x between its starting point and the next discrete interaction point or a boundary to the nearest adjacent physical region or a point of leakage from the absorber is subdivided into **steps** s such that at every step the following conditions are fulfilled (***in the simplest approach***):

1. Mean ionization energy loss $\Delta E = abs\left(\frac{dE}{dx}\right) \times s$ is small ($\frac{\Delta E}{E} \sim 1 - 5\%$)
2. Angle due to Multiple Coulomb scattering is small ($\theta_{plane} \leq \sim 0.1$ mrad)

$$\theta_0 = \theta_{plane}^{rms} = \frac{1}{\sqrt{2}}\theta_{space}^{rms}$$

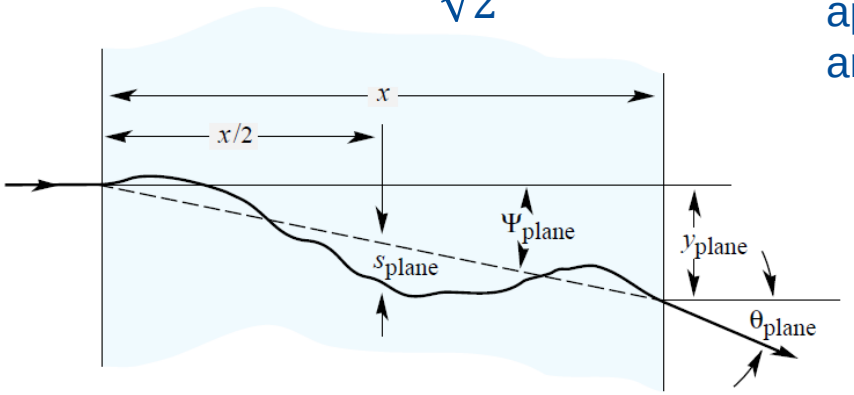

It is sufficient for many applications to use a Gaussian approximation for the central 98% of the projected angular distribution with an RMS given by:

$$\theta_0 = \frac{0.0136GeV}{\beta p} z \sqrt{\frac{x}{X_0}} [1 + 0.038 \ln(x\, z^2/X_0\beta^2)]$$

where z, β and p are the particle charge number, velocity and momentum and X_0 is the medium radiation length

Ionization and Radiative Energy Loss dE/dx

Continuous-slowing-down-approximation (CSDA)

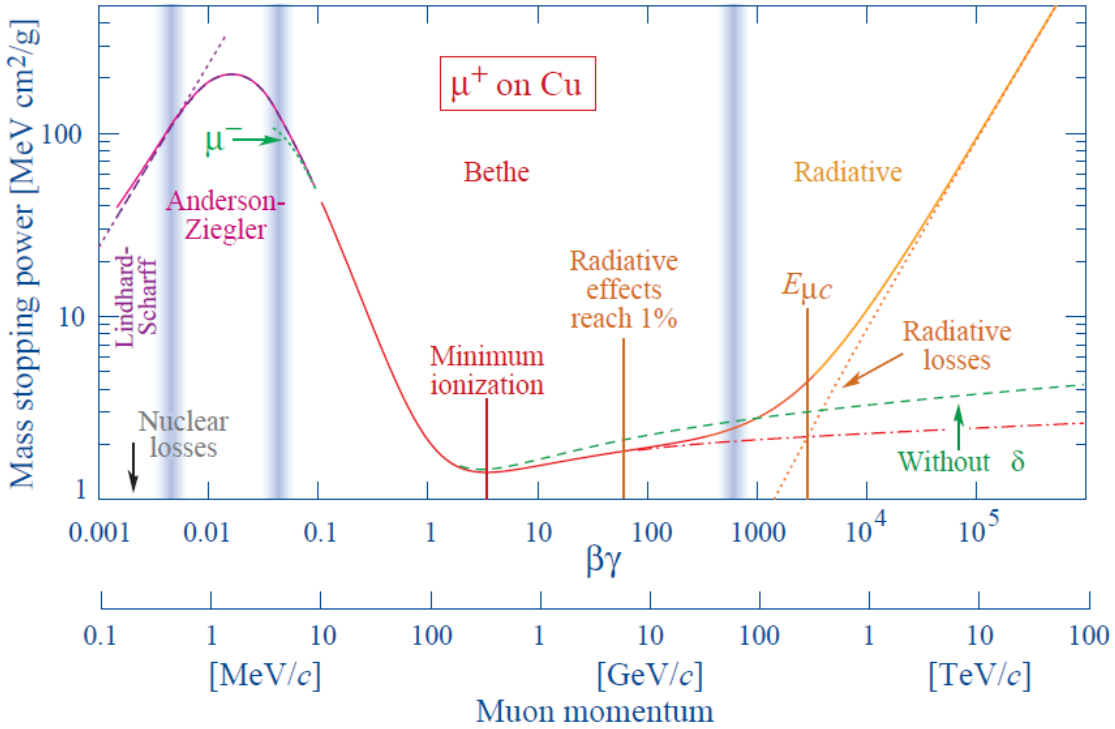

$$\gamma = \frac{1}{\sqrt{1-\beta^2}} = \frac{E_t}{m}$$

$$\beta\gamma = \sqrt{\gamma^2 - 1}$$

$$\beta = \frac{v}{c} = \frac{\beta\gamma}{\gamma} = \frac{p}{E_t}$$

Mean stopping power for charged particles: (-dE/dx) = a (E) + b (E)E, where a (E) is the electronic stopping power, and b (E) is due to radiative processes – bremsstrahlung, pair production and photonuclear interactions; both a (E) and b (E) are slowly varying functions of E at high energies

Mean Stopping Power

$$-\frac{1}{\rho}\frac{dE}{dx} = 4\pi N_A r_e^2 m_e c^2 z^2 \frac{Z}{A}\frac{1}{\beta^2} L(\beta)$$

$$L(\beta) = L_0(\beta) + \sum_i \Delta L_i$$

$$L_0(\beta) = \ln\left(\frac{2m_e c^2 \beta^2 \gamma^2}{I}\right) - \beta^2 - \frac{\delta}{2}$$

Bethe-Bloch formula

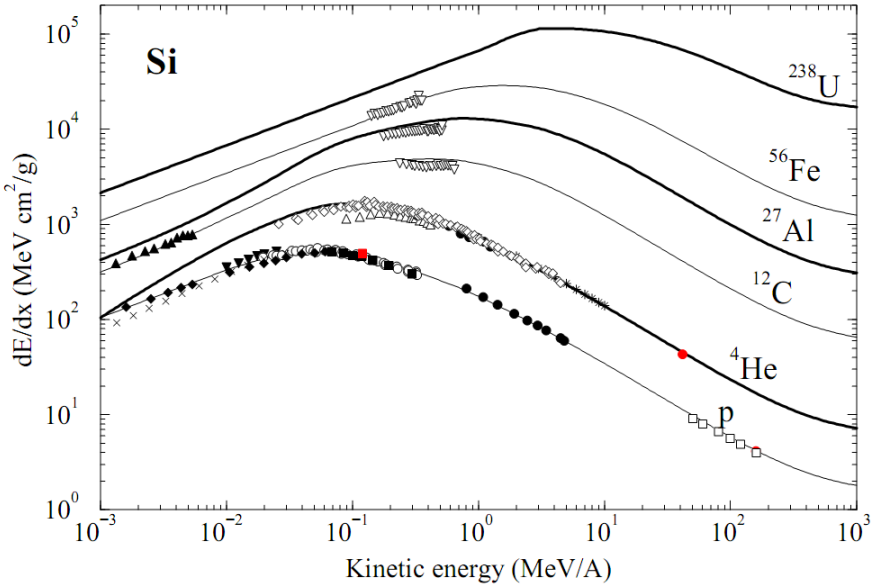

ΔLi: (i) **Lindhard-Sørensen** correction (exact solution to the Dirac equation; terms higher than z^2);

(ii) **Barkas** correction (target polarization effects due to low-energy distant collisions);

(iii) **shell** correction;

Projectile **effective charge** comes separately as a multiplicative factor that takes into account electron capture at low projectile energies (e.g., z_{eff} ~ 20 for 1-MeV/A ^{238}U in Al, instead of bare charge of 92).

Fermilab

dE/dx: Mixtures and Heavy Ions

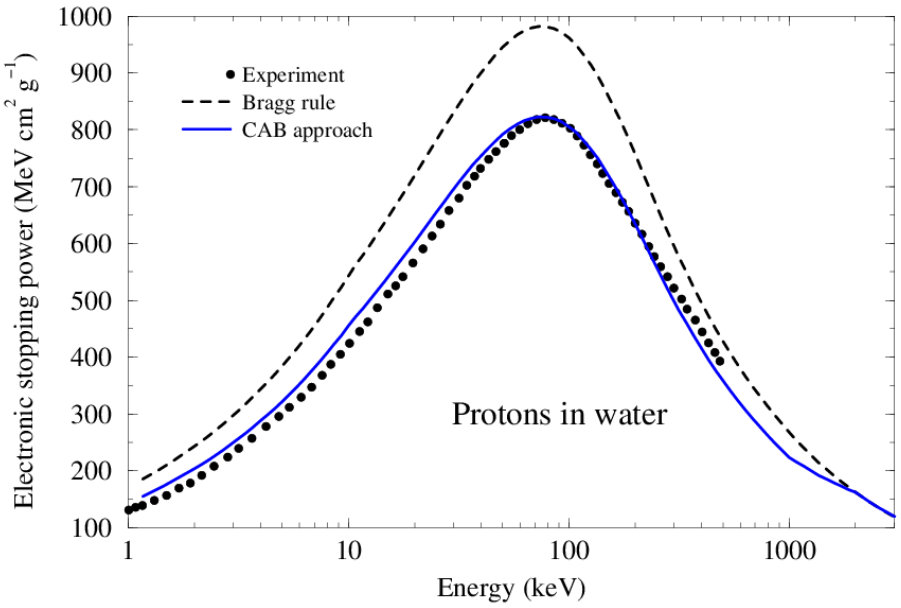

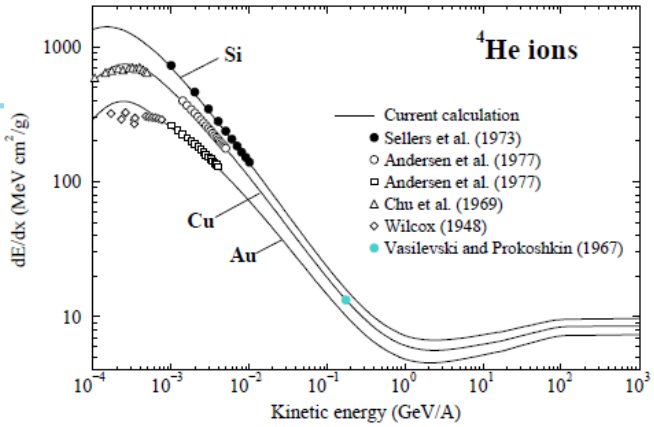

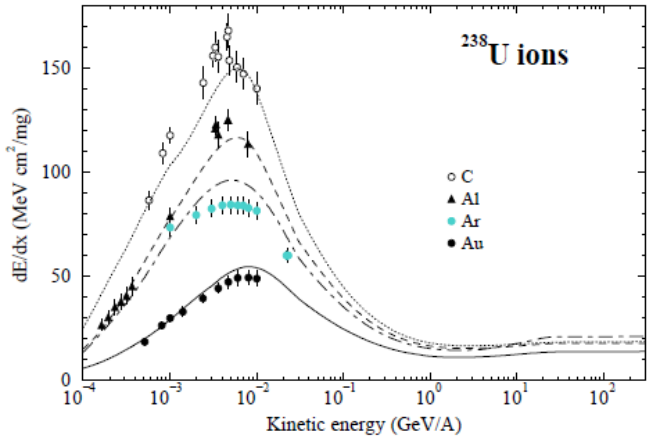

Stopping power of ions in compounds usually is described according to Bragg's rule. At low energies and for low-Z materials the difference between measured and predicted dE/dx can be as large as 20%. The "cores-and-bonds" (CAB) method in MARS15 takes into account chemical bonds fitted to experiment for various compounds

Energy Loss and Energy Deposition Modeling

1. The CSDA dE/dx is widely used in quick estimations of energy loss by particle beams and in simplified simulations of energy loss and energy deposition along the charged particle tracks in hadronic and electromagnetic cascades.
2. In a more sophisticated approach used these days in several codes, precise modeling of knock-on electron production with energy-angle correlations taken into account is done for electronic losses.

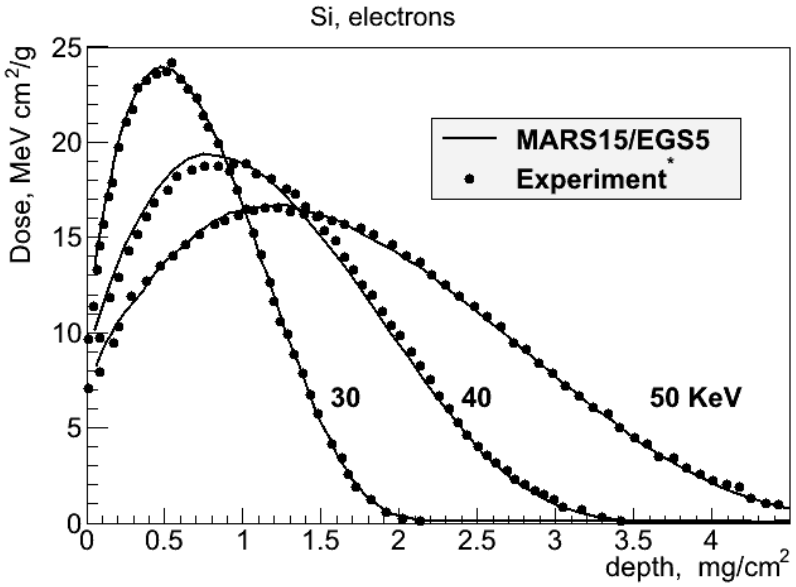

3. Radiative processes – bremsstrahlung, pair production and inelastic nuclear interactions (via virtual photon) – for muons and high-energy hadrons - are modelled exclusively using pointwise x-sections.

Items (2) and (3) allow precise calculation of 3D energy deposition maps induced by high energy cascades.

Modelling in the State-of-the-Art MC Codes

- The radiative processes for high-energy muons and charged hadrons (direct e^+e^- pair production, bremsstrahlung and nuclear interaction *via* a virtual photon) as well as large $\frac{\Delta E}{E}$ ionization energy losses in "hard" collisions (see next slide) are modelled as discrete interactions.
- The large-angle ("Moliere") Coulomb scattering is modelled via sophisticated algorithms, in some cases with energy-angle correlations taken into account.
- Customized steppers (*e.g.*, 8th order Runge-Kutta solver) are used for charged particle tracking in complex geometry with complex magnetic and electric fields.
- Decays of unstable charged and neutral particles are modelled on a step either analogously or with one of the variance reduction techniques (modified decay length or forced decays).

Correlated Energy Loss and Coulomb Scattering (1)

An advanced way to simulate multiple scattering is based on a separate treatment of "soft" and "hard" interactions. Angular deflection in a large number of "soft" collisions is sampled from a "continues" distribution with "hard" scattering simulated explicitly. There is an obvious correlation between precision and efficiency of the algorithm and the value of a boundary angle θ_b between "soft" and "hard" collisions. For small θ_b, a number of discrete interactions is large and precision is high, for large θ_b, the efficiency increases but the accuracy decreases. In SAMCS of MARS15, "continues" angular distribution is described as

$$F_c(\theta,t)=\frac{1}{\pi<\theta_s^2>}e^{-\phi_s}(1+r_sL_2(\phi_s)+3r_s^2L_4(\phi_s)+\cdots),$$

where $\phi_s=\frac{\theta^2}{<\theta_s^2>}, r_s=\frac{<\theta_s^4>}{2<\theta_s^2>^2}, <\theta_s^k>=t\int_0^{\theta_b}\theta^k\frac{d\Sigma}{d\Omega}d\Omega,$ where L_k are Laguerre polynomials and *t* is the pathlength.

"Continues" energy loss distribution are described by a modified Vavilov distribution. Simulation of "hard" collisions takes into account projectile and nucleus formfactors (charge distributions) and exact kinematics of a projectile-electron interactions. The boundary angle θ_b is defined, providing a precise sampling of scattering angle and energy loss and a small number of "hard" collisions.

Correlated Energy Loss and Coulomb Scattering (2)

Energy loss distributions of 200 MeV/c muons after a pathlength of 1cm (left) and 30cm (right) of liquid hydrogen

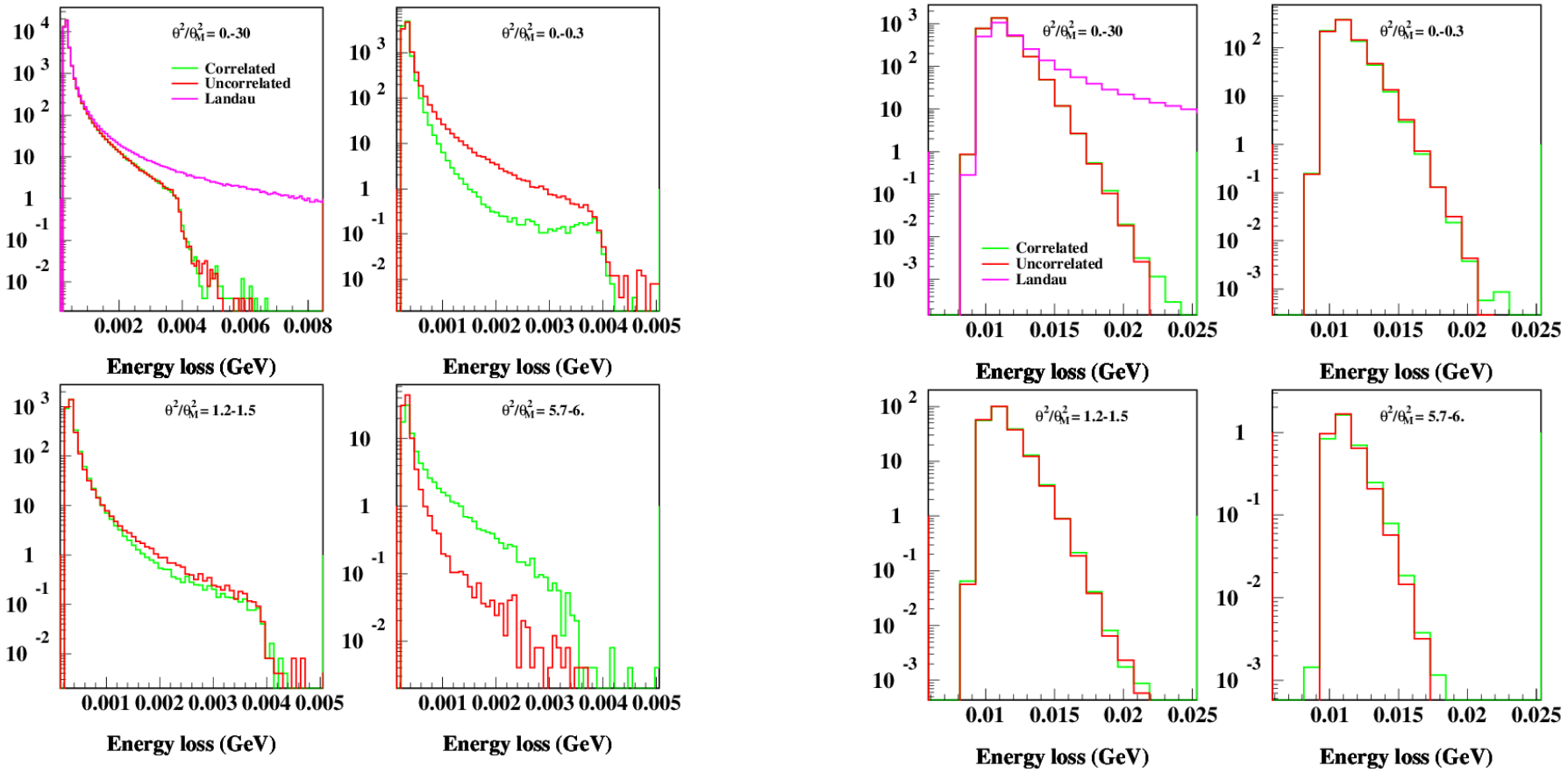

➔ **Energy-angle correlations are especially important for simulations in tiny accelerator and detector components**

Fermilab

Three-Body Decays

Matrix element & polarization added to basic decay kinematics of kaons and muons

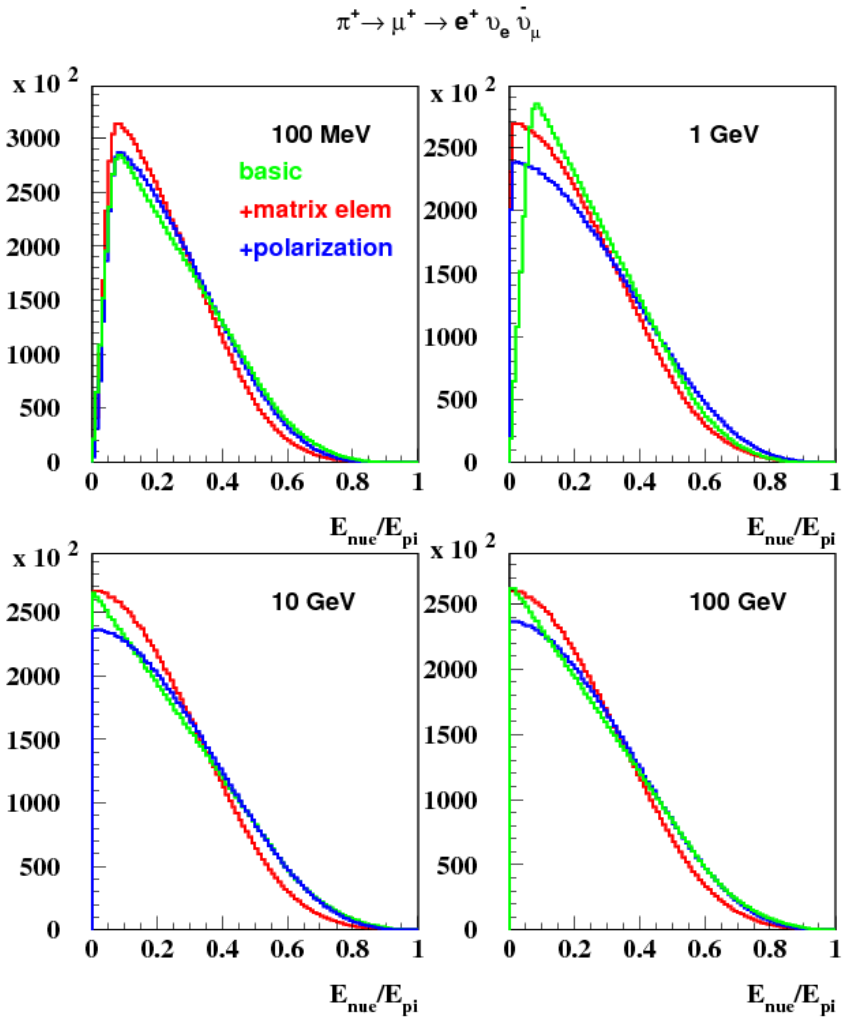

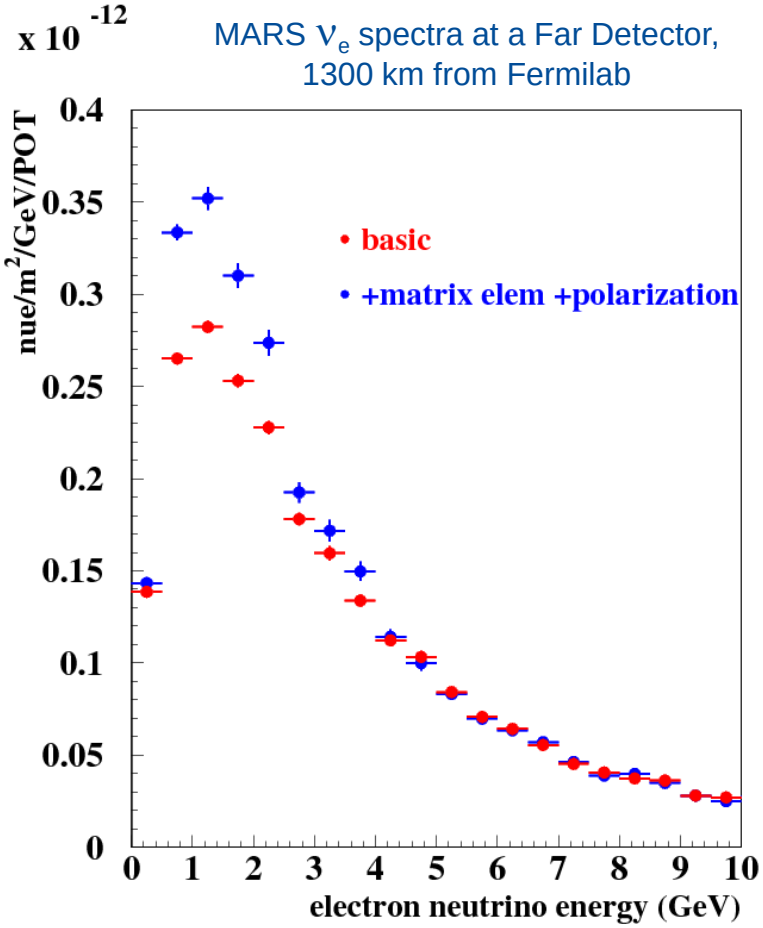

Fermilab